FINAL DESIGN FOR THE bERLinPro MAIN LINAC CAVITY *

A. Neumann†, J. Knobloch
Helmholtz-Zentrum Berlin, 12489 Berlin, Germany
B. Riemann, T. Weis
TU Dortmund University, Dortmund, Germany
K. Brackebusch, T. Flisgen, T. Galek, U. van Rienen
Rostock University, Rostock, Germany

Abstract

The Berlin Energy Recovery Linac Project (bERLinPro) is designed to develop and demonstrate CW LINAC technology for 100-mA-class ERLs. High-current operation requires an effective damping of higher-order modes (HOMs) of the 1.3 GHz main-linac cavities. We have studied elliptical 7-cell cavities based on a modified Cornell ERL design combined with JLab's waveguide HOM damping approach. This paper will summarize the final optimization of the end-cell tuning for minimum external Q of the HOMs, coupler kick calculations of the single TTF fundamental power coupler (FPC) as well as multipole expansion analysis of the given modes and a discussion on operational aspects.

INTRODUCTION

For the bERLinPro ERL [1] a 100 mA beam has to be accelerated and decelerated in the main linac of the recirculator from 6.5 MeV to 50 MeV and vice versa while preserving a low normalized emittance of smaller than 1 mm mrad. Effectively the linac cavities therefore experience the passage of two with respect to the TM_{010}-π mode 180 deg. phase shifted high current beams. Thus strong HOM damping is required in order to avoid beam break-up instability (BBU) [2] by the interaction with dipole-like mode patterns excited by the beam during previous passages. By that the cavity design has to be optimized for low transverse shunt impedance $R/Q_\perp$ and low external quality factors Q_{ext} regarding the HOMs, while the fundamental has to feature low peak field ratios and a high shunt impedance. This challenge was addressed by combining Cornell's mid-cell shape [3] featuring low E_{peak}/E_{acc}, thus avoiding field emission, with JLabs concept of waveguide damped cavity structures [4]. The latter has a natural cutoff frequency by the waveguide dimensions and the danger of dust propagating from ferrite-based beam tube absorbers is avoided.

Figure 1 shows a sketch of the bERLinPro demonstrator ERL and the main linac cavity design. By two Y-shaped waveguide (WG) end groups rotated by 60 deg. any HOM's polarization is covered. To even improve the propagation of the HOMs, the beam tube is enlarged from the 72 mm iris to 105 mm via a spline based nose cone transition. Table 1 summarizes the calculated RF performance of the cavity. The structure was developed and optimized within a collaboration of the universities Dortmund and Rostock with HZB. The methods applied and developed for this project are published in [5–9].

Table 1: Calculated RF parameters and operating conditions of the main Linac cavity with a TTF-III FPC and five HOM damping rectangular waveguides.

Number of cells	7
$R/Q_\parallel$	788 Ω
$f_{TM_{010}-\pi}$	1.3 GHz
E_{peak}/E_{acc}	2.08
B_{peak}/E_{acc}	4.4 mT/MVm^{-1}
Q_{ext} TM_{110} dipole	$\leq 8 \cdot 10^3$
Beam tube TE_{01} cutoff	1.596 GHz
Waveguide TE_{10} cutoff	1.576 GHz
Q_L for TM_{010}-π	$1 \cdot 10^7 - 1 \cdot 10^8$
$P_{forward}$ at $Q_L = 5 \cdot 10^7 (\Delta f = 0)$	1.4 kW

Recently [10] end-cell tuning optimizations using CST MWS's [11] swarm particle optimizer with the eigenmode solver were performed to achieve best HOM damping results while still keeping the cavity field-flat and within given limits regarding peak field ratios and $R/Q_\parallel$. The best candidate of this approach was selected for more detailed studies, presented here, in order to achieve a design ready for production.

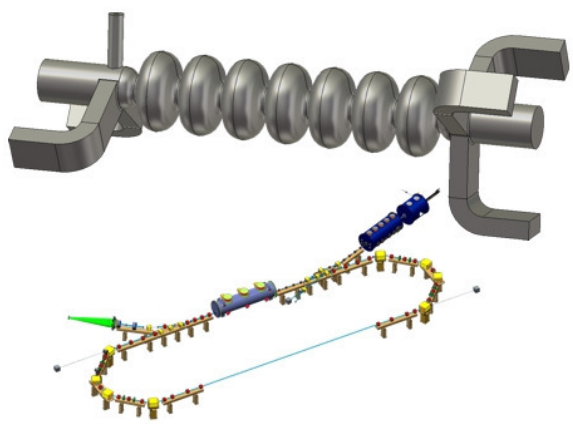

Figure 1: Scheme of the bERLinPro ERL with the main linac section within the recirculating ring. Above the linac cavity structure is shown including the FPC and five waveguides for HOM damping.

* Work supported by German Bundesministerium für Bildung und Forschung, Land Berlin, by grants of Helmholtz Association and by Federal Ministry for Research and Education BMBF under contract 05K10HRC and 05K10PEA
† Axel.Neumann@helmholtz-berlin.de

Copyright © 2014 CC-BY-3.0 and by the respective authors

ISBN 978-3-95450-142-7

HOM DAMPING CONCEPT AND PERFORMANCE

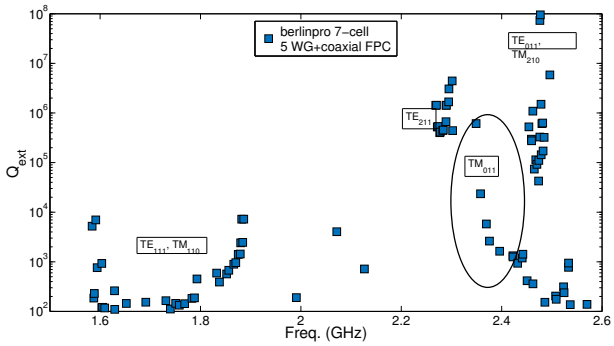

Figure 2: External Q for the 7-cell bERLinPro linac cavity featuring one coaxial FPC and five waveguide based HOM absorbers obtained by CST MWS eigenmode computations.

As it was demonstrated [12], that CW-driven cavities without beam-loading can be driven up to loaded Q of $2{\cdot}10^8$, one WG was replaced by a variable CW-modified TTF-III coupler for a coupling range given in Table 1. Figure 2 shows the achieved HOM damping of the final model. The dipole modes are strongly damped, whereas TM quadrupole modes show a partly localization within the inner cells leading to higher Q_{ext}. Transverse $R/Q_\perp$ calculations by directly integrating the Lorentz forces of the on-axis field components, a multipole decomposition and multi-integration path analysis [6, 7] have shown, that high Q_{ext} m≥2 modes may have dipole-like on-axis field components.

Breaking the Symmetry with the Coaxial FPC

A reason for this might be the broken symmetry by insertion of the coaxial FPC. To tackle this problem, calculations were done comparing for different FPC penetration depth with an all WG system having the full symmetry. The outcome with respect to the BBU parameter $R/Q_\perp \cdot Q_{\text{ext}}$ is displayed in Figure 3. The current threshold is given by a dipole component of a quadrupole mode. This on-axis $R/Q_\perp > 0$ seems to be also common for the full WG system, but is stronger for the coaxial antenna, such that a compensating stub might has to be inserted.

Further, a localized mode with a strong dipole kick appears between the cavity iris and the WG structure, as shown in Figure 4. To avoid this, being the second strongest candidate limiting the threshold current, the whole end-group has to be reworked by inserting shapes similar to [4].

Finally, as all calculations needed to be done within 3D and computational time and power limits the accessible spectrum, a limited convergence study was started to overcome numerical outliers. In Figure 5 the result demonstrates, that the first dipole bands reached convergence, but that there are still variations within the second monopole band and first TE/TM quadrupole band, where the latter directly influences the BBU limit as for now. More studies with respect to that topic are underway.

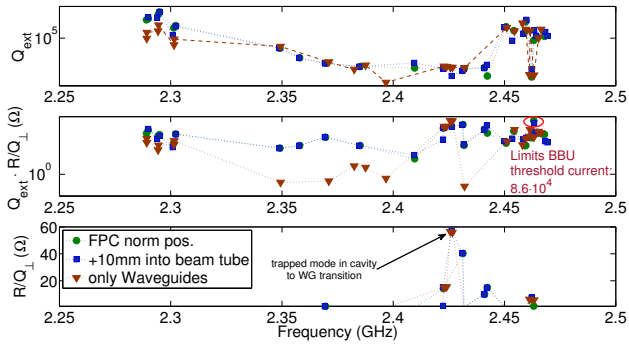

Figure 3: Comparison of Q_{ext}, $R/Q_\perp$ and the BBU parameter $R/Q_\perp \cdot Q_{\text{ext}}$ for the TTF FPC at nominal position (green dots), 10 mm more into the beam tube (blue squares) and a symmetric system with six waveguides.

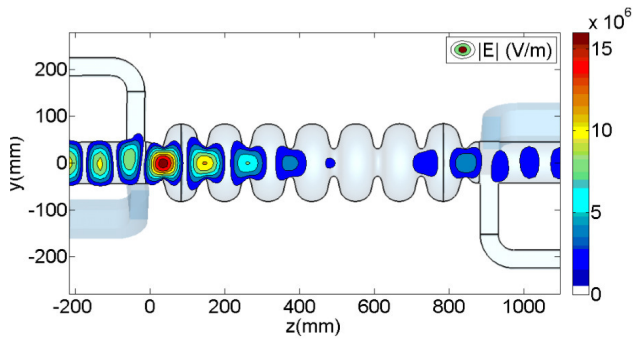

Figure 4: Localized mode within the iris to Y-shaped waveguide section at 2.4 GHz bearing a strong dipole kick on the beam.

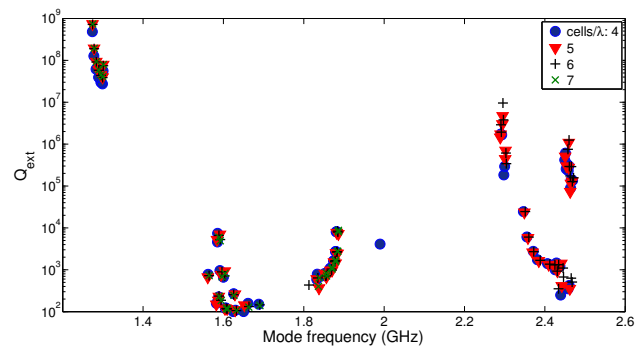

Figure 5: Convergence study of Q_{ext} for the HOM spectrum using different mesh densities with the hexahedral mesh of CST 2014 using *eight cells per max model box edge*.

Copyright © 2014 CC-BY-3.0 and by the respective authors

ISBN 978-3-95450-142-7

Table 2: Beam and cavity parameters for the coupler kick calculations.

$\epsilon_{n,y,x}$	1 mm mrad
σ_t	5 ps rms
$\sigma_{y,x}$	≈0.7 mm rms
$I_{avg,beam}$	100 mA
$E_{kin,ini}$	6.5 MeV
V_{acc}	15 MV
E_{acc}	18.56 MV/m
Φ_{acc}	-20 to 20 deg

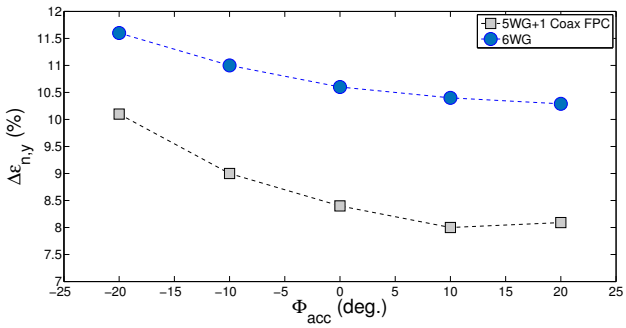

Figure 6: Relative emittance growth in the vertical planes versus ϕ_{acc} for the 5WG+coax FPC structure and the 6WG cavity in reference to the bare cavity using the PIC code.

Coupler Kick and Emittance Dilution Calculations

In addition to coupler kick effects on the HOM, it has to be studied whether the 6.5 MeV beam is subject to coupler kick and emittance increase within the linac cavities by the fundamental mode. Using the bunch parameters given in Table 2 kick calculations with the CST PIC tracking solver as described in [13] were performed at nominal field level for a given range of accelerating phases comparing the coaxial FPC design with the full WG structure (without space charge). As displayed in Figure 6 the emittance increase for standing wave regime, as the cavity is operated at zero net beam-loading under non-matching conditions, is nearly 10% for the coaxial FPC and 5WG design. The corresponding fields are shown in Figure 7. The evolution of the emittance in both transverse planes is given in Figure 8. As it only happens to take place within the coaxial FPC's plane, also here the need for a compensating stub or similar is demonstrated. But still the full WG solution shows a stronger emittance dilution, even in both planes.

SUMMARY

The design is closing in to be finalized for production. Main emphasis has to be put now on the end-groups and more in depth and multipole analysis has to be applied in order to understand the coupler kick effect on the HOMs.

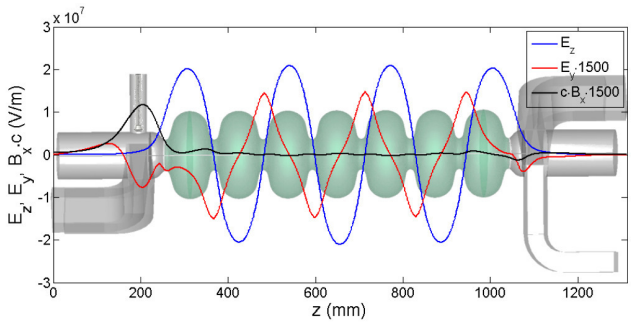

Figure 7: On-axis longitudinal and transverse field components for an electric wall boundary condition for the standing wave regime.

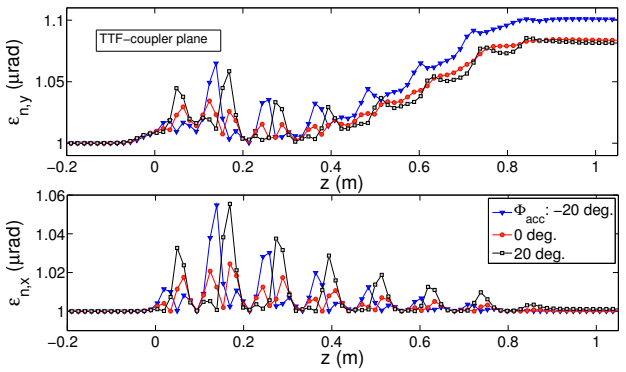

Figure 8: Emittance evolution in both transverse planes for the bERLinPro design.

ACKNOWLEDGMENTS

The authors acknowledge the helpful discussion with Robert Rimmer and Haipeng Wang from JLab as well as Frank Marhauser from muons inc. about cavity and HOM absorber design issues.

Copyright © 2014 CC-BY-3.0 and by the respective authors

ISBN 978-3-95450-142-7

REFERENCES

[1] J. Knobloch et al., ICFA Beam Dynamics Newsletters, No.58, p. 118, August 2012.

[2] G.H. Hoffstaetter, I.V. Bazarov, and Ch. Song., Phys. Rev. ST Accel. Beams, 10:044401, Apr 2007.

[3] N. Valles et al., IPAC'10, Tsukuba, 2010, WEPEC068, p. 3046 ff.

[4] F. Marhauser et al., EPAC'08, Genoa, 2008, MOPP140, p. 886 ff.

[5] B. Riemann et al., ICAP'12, Warnemünde, 2012 WEP14, p. 167 ff.

[6] A. Neumann et al., ICAP'12, Warnemünde, 2012 FRAAC03, p. 278 ff.

[7] B. Riemann et al., LINAC'12, Tel Aviv, 2012, MOPB066, p. 330ff.

[8] A. Neumann et al., LINAC'12, Tel Aviv, 2012, MOPB067, p. 333ff.

[9] T. Galek et al., IPAC'13, Shanghai, 2013, WEPWO010, p. 2331ff.

[10] T. Galek et al., IPAC'14, Dresden, 2014, MOPME017, p. 412ff.

[11] CST AG, Microwave Studio®, Darmstadt, Germany.

[12] A. Neumann et al., SRF'11, Chicago, 2011, MOPO067, p. 262 ff.

[13] A. Neumann et al., IPAC'14, Dresden, 2014, WEPRI007, p. 2490ff.

Copyright © 2014 CC-BY-3.0 and by the respective authors